Investigation on the Properties of the Mixture Consisting of $Mg(NH_2)_2$, LiH, and $LiBH_4$ as a Hydrogen Storage Material

Jianjiang Hu,[†,‡] Maximilian Fichtner,*[,†] and Ping Chen[‡]

Institute for Nanotechnology, Forschungszentrum Karlsruhe, Postfach 3640, D-76021 Karlsruhe, Germany, and Department of Physics, National University of Singapore, Singapore 117542

Received August 4, 2008. Revised Manuscript Received September 10, 2008

A maximum hydrogen amount of 9.1 wt % was obtained at 300 °C from the $1Mg(NH_2)_2-2LiH-0.67LiBH_4$ system. Various analyses and thermodynamic calculations revealed that the MgH_2 and $LiNH_2$ can be readily converted to $Mg(NH_2)_2$ and LiH at 120 °C in the presence of $LiBH_4$. A comparison between the sample $1Mg(NH_2)_2-2LiH-1LiBH_4$ and the ternary mixture $1MgH_2-2LiNH_2-1LiBH_4$ indicated that both samples behave very similarly in hydrogen desorption, thermal effects, and chemical changes during dehydrogenation.

Introduction

The safe and efficient storage of hydrogen is widely recognized as one of the key technological challenges in the transition toward a hydrogen economy.[1] Compared to the physical approaches such as high pressure compression and liquefaction via cryogenics, hydrogen storage in the solid state has among others the merits of high volumetric and gravimetric hydrogen density,[2] which is paramount for mobile application.

The chemical approach toward hydrogen storage has been extensively explored in the past decades. Although the hydrogen storage medium was focused on metal hydrides or Al-based complex hydrides previously,[3,4] attempts are being made in recent years with metal−nitrogen−hydrogen systems.[5−8] The introduction of nitrogen into the hydrogen storage system was revitalized by the finding in 2002 that a large amount of hydrogen can be chemically absorbed by metal nitrides.[5] The use of metal−nitrogen compounds as a hydrogen source expands the scope of materials selection. Usually the combination of $H^{\delta-}$ in hydrides and $H^{\delta+}$ in amides results in faster dehydrogenation kinetics because of the favorable energy relationship.[9] A variety of metal amide−hydride combinations have thus been designed and investigated for their hydrogen sorption performances by applying this strategy.[10]

Compared to many investigations that start with a binary mixture consisting of a metal amide and a metal hydride, Yang et al. used a ternary mixture system (TMS) comprising an amide ($LiNH_2$), a borohydride ($LiBH_4$), and a metal hydride (MgH_2).[11−13] At a 1:2:1 MgH_2:$LiNH_2$:$LiBH_4$ (TMS-I) molar ratio, this ternary mixture system was found to possess hydrogen desorption performance superior to any single component or two combination from the three starting materials. Faster kinetics and a lower level of NH_3 generation were found.[11] Interestingly, the hydrogen desorption in the low temperature range of the ternary mixture occurred via the following reaction

$$Mg(NH_2)_2 + 2LiH \rightarrow Li_2Mg(NH)_2 + 2H_2 \qquad (1)$$

although the starting materials were $LiNH_2$, $LiBH_4$, and MgH_2. This implies that a conversion from $LiNH_2$ and MgH_2 to $Mg(NH_2)_2$ and LiH may have occurred during the hydrogen desorption.

Starting with $LiNH_2$ and MgH_2, Luo and Rönnebro obtained $Mg(NH_2)_2$ and LiH after one cycle of dehydrogenation and rehydrogenation and proposed the following conversion reaction[14]

* Corresponding author. Phone: 49 (0)7247825340. Fax: 49 (0)7247826368. E-mail: maximilian.fichtner@kit.edu.
[†] Forschungszentrum Karlsruhe.
[‡] National University of Singapore.

(1) Schlapbach, L.; Züttel, A. *Nature* **2001**, *414*, 353–358.
(2) Schüth, F.; Bogdanović, B.; Felderhoff, M. *Chem. Commun.* **2004**, 2249–2258.
(3) Grochala, W.; Edwards, P. P. *Chem. Rev.* **2004**, *104*, 1283–1315.
(4) Bowman, R. C.; Fultz, B. *MRS Bull.* **2002**, *27* (9), 688–693.
(5) Chen, P.; Xiong, Z. T.; Luo, J. Z.; Lin, J. Y.; Tan, K. L. *Nature* **2002**, *420* (6913), 302–304.
(6) Xiong, Z. T.; Wu, G. T.; Hu, H. J.; Chen, P. *Adv. Mater.* **2004**, *16* (17), 1522–1525.
(7) Luo, W. *J. Alloys Compd.* **2004**, *381*, 284–287.
(8) Leng, H. Y.; Ichikawa, T.; Hino, S.; Nakagawa, T.; Fujii, H. *J. Phys. Chem. B* **2005**, *109*, 10744–10748.
(9) Lu, J.; Fang, Z. Z.; Sohn, H. Y. *Inorg. Chem.* **2006**, *45*, 8749–8754.
(10) Chen, P.; Xiong, Z. T.; Wu, G. T.; Liu, Y.; Hu, J. J.; Luo, W. F. *Scr. Mater.* **2007**, *56*, 817–822.
(11) Yang, J.; Sudik, A.; Siegel, D. J.; Halliday, D.; Drews, A.; Carter III, R. O.; Wolverton, C.; Lewis, G. J.; Sachtler, J. W. A.; Low, J. J.; Faheem, S. A.; Lesch, D. A.; Ozolins, V. *J. Alloys Compd.* **2007**, *446−447*, 345–349.
(12) Lewis, G. J.; Sachtler, J. W. A.; Low, J. J.; Lesch, D. A.; Faheem, S. A.; Dosek, P. M.; Knight, L. M.; Halloran, L.; Jensen, C. M.; Yang, J.; Sudik, A.; Siegel, D. J.; Wolverton, C.; Ozolins, V.; Zhang, S. *J. Alloys Compd.* **2007**, *446−447*, 355–359.
(13) Yang, J.; Sudik, A.; Siegel, D. J.; Halliday, D.; Drews, A.; Carter III, R. O.; Wolverton, C.; Lewis, G. J.; Sachtler, J. W. A.; Low, J. J.; Faheem, S. A.; Lesch, D. A.; Ozolins, V. *Angew. Chem., Int. Ed.* **2008**, *47*, 882–887.
(14) Luo, W.; Rönnebro, E. *J. Alloys Compd.* **2005**, *404−406*, 392–395.

10.1021/cm802129b CCC: $40.75
Published on Web 10/24/2008

$$MgH_2 + 2LiNH_2 \rightarrow Li_2Mg(NH)_2 + 2H_2 \leftrightarrow Mg(NH_2)_2 + 2LiH \quad (2)$$

The authors in ref 11 found that $LiNH_2$ and $LiBH_4$ in the mixture first formed a quaternary hydride $Li_4(BH_4)(NH_2)_3$, which reacted with MgH_2 and released hydrogen. The resulted $Li_2Mg(NH)_2$ functioned as seeds that could reportedly enhance the hydrogen desorption reaction via reaction 1. Later, optimization was made by Lewis et al. by applying the combinatorial synthesis and screening techniques on the TMS.[12] The optimum composition was found to be $0.6LiNH_2-0.3MgH_2-0.1LiBH_4$ with a reversible capacity of about 3.4 wt % at 220 °C. It was found that this TMS was a self-catalyzed reaction very recently by Yang et al. [13]

Among the Metal−N−H systems, Li−Mg−N−H system comprising LiH and $Mg(NH_2)_2$ with its 5.6% reversible capacity is so far the most promising system with good reversibility and moderate operation temperatures.[6−8] Our recent work on the improvement of $Mg(NH_2)_2$−LiH at a 1:2 molar ratio showed that the kinetics in the hydrogen desorption and absorption of the system was enhanced significantly by adding small amount of $LiBH_4$.[15] About 5 wt % hydrogen could be released at 140 °C and recharged at 100 °C with a kinetics three times as fast as the system without $LiBH_4$ addition. The concomitant NH_3 generation was also found lower than from the pristine Li−Mg−N−H system. The formation of the quaternary hydride of $Li_4(BH_4)(NH_2)_3$ was detected in the materials as well after dehydrogenation and rehydrogenation. Similar to the above-mentioned TMS-I, hydrogen desorption at about 300 °C was observed following a major dehydrogenation at about 170 °C. Therefore, the $LiBH_4$ modified $Mg(NH_2)_2$−LiH system (TMS-II) could be an analogue to $MgH_2 + 2LiNH_2 + LiBH_4$ (i.e., TMS-I).

We are therefore interested to know the hydrogen desorption properties of the $Mg(NH_2)_2$−LiH system as a function of $LiBH_4$ content. $LiBH_4$ will be introduced in this study to the typical $Mg(NH_2)_2$−LiH (1:2 molar ratio) system as a component rather than as an additive with a small amount.

Experimental Section

Sample Preparation. $Mg(NH_2)_2$ (>95%, synthesized in-house), LiH (95%, Sigma-Aldrich), MgH_2 (Alfa Aesar, 98%) and $LiBH_4$ (95%, Sigma-Aldrich) were stored in a glovebox with Ar as protecting atmosphere and used as received without any pretreatment. For the ball-milling process, the starting chemicals were loaded into a milling vessel inside the glovebox. Ball milling was conducted on a Retsch PM400E at 200 rpm for 36 h. Samples of $[1Mg(NH_2)_2 + 2LiH + xLiBH_4]$ with $x = 0.3$, 0.5, 0.67, and 1.0 were prepared, respectively. The ternary mixture consisting of $MgH_2-LiNH_2-LiBH_4$ at 1:2:1 molar ratio (TMS-I) in ref 11 was also prepared under the same conditions for comparison purpose.

Characterization Methods. Temperature-programmed desorption (TPD) tests were carried out on a home-built apparatus. About 100 mg of sample was loaded into a tube reactor housed in a tubing furnace. Purified Ar was used as purge gas, which flowed into a thermal conductivity detector. The evolution of H_2 from samples by heating causes increase in thermal conductivity which was recorded. The heating rate was kept at 2 °C/min for all tests. Details about the apparatus have been described elsewhere.[16] The volumetric desorption measurements were performed on a commercial Sieverts' gas reaction system from Advanced-Materials Corp, USA. About 300 mg of sample was used each time. The measurement was conducted in an automatic release mode, during which the whole system was first evacuated. The hydrogen was released to the vacuum. The reactor was heated at a heating rate of 2 °C/min. The measurements of Fourier transform infrared spectroscopy (FTIR) were conducted on a Perkin Elemer FTIR-3000 Spectrometer. The powdery samples were loaded into the in situ cell in the glovebox and measured at a resolution of 4 cm^{-1}. For the X-ray diffractometry (XRD) measurements (Bruker D8-advance X-ray diffractometer with Cu Kα radiation), about 50−70 mg of sample was pressed into pellets and fixed to the XRD sample holder, which was housed inside a protective hood operating under a vacuum. differential scanning calorimetry (DSC) measurements were performed on a Netzsch DSC 204 HP housed inside the glovebox. Samples were heated at 2 °C/min under the flow of purified Ar at 30 mL/min.

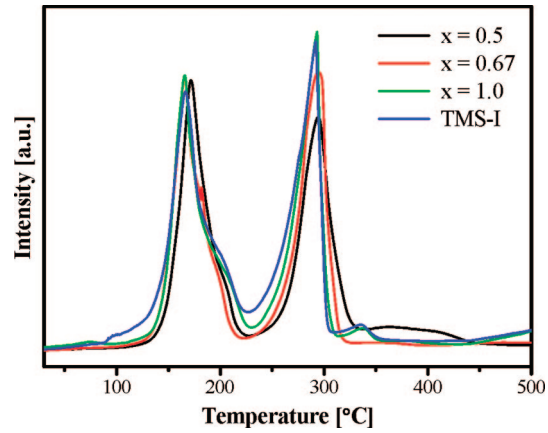

Figure 1. TPD curves of the as-milled samples.

Results and Discussion

Influence of $LiBH_4$ Content on Hydrogen Desorption Amount. The qualitative characterization of the hydrogen desorption behavior by the TPD tests displayed two major distinct peaks for all the samples (Figure 1). The peak areas or the hydrogen desorption amounts in the low-temperature range seemed not very much affected by the addition of $LiBH_4$. In the high-temperature range, however, the amount of hydrogen desorption presented a complicated feature. The peak area increased obviously as the x value increased from 0.5 to 0.67. For the TMS-I and TMS-II, similar peak areas and shapes were observed. The simultaneous monitoring of NH_3 generation during TPD showed low levels of NH_3 generation for all the samples in the first dehydrogenation step. However, a drastic increase in NH_3 was observed in the second dehydrogenation step for the sample at $x = 1$ and the sample $1MgH_2-2LiNH_2-1LiBH_4$ (Figure 2).

The quantitative measurements of the hydrogen desorption on the Sieverts' system (Figure 3) showed two steps of hydrogen release, consistent with the TPD results. In addition, the relative hydrogen amount in respect to the

(15) Hu, J. J.; Liu, Y.; Wu, G.; Xiong, Z.; Chua, Y. S.; Chen, P. *Chem. Mater.* **2008**, *20* (13), 4398–4402.

(16) Chen, P.; Xiong, Z. T.; Luo, J. Z.; Lin, J. Y.; Tan, K. L. *J. Phys. Chem. B* **2003**, *107*, 10967–10970.

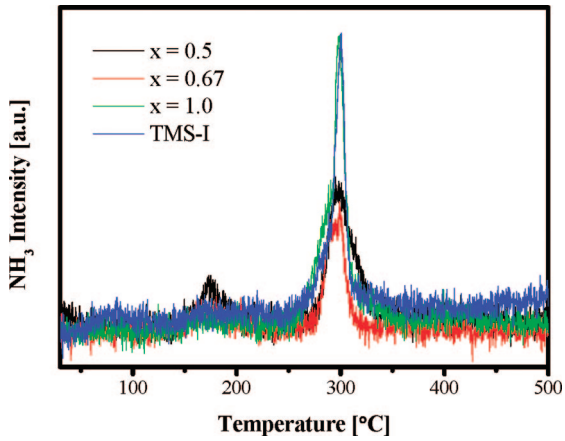

Figure 2. Simultaneous ammonia monitoring by mass-spectrometer during TPD test.

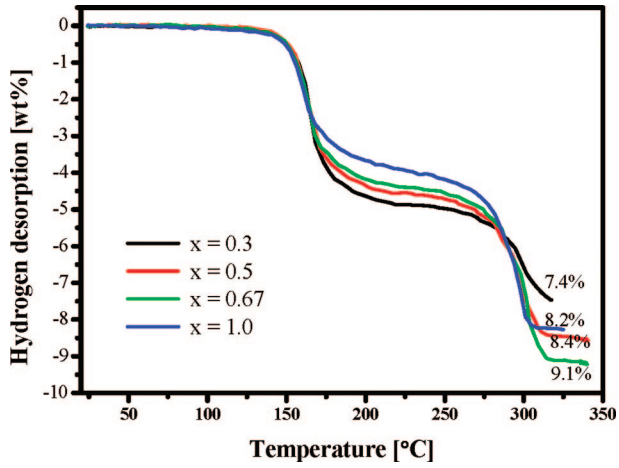

Figure 3. Volumetric measurements of samples with various $LiBH_4$ contents.

various $LiBH_4$ contents was clearly reflected: the highest hydrogen desorption amount was obtained with lowest $LiBH_4$ content ($x = 0.3$ in this study) in the low temperature range. This suggests that $LiBH_4$ did not participate in first hydrogen desorption reaction and its addition simply lowered the capacity of the system.

The second hydrogen desorption occurred between $LiBH_4$ and the resulting $Li_2Mg(NH)_2$ from the first step. The reaction was proposed as follows in ref 13

$$Li_2Mg(NH)_2 + \frac{2}{3}LiBH_4 \rightarrow \frac{2}{3}Li_3BN_2 + \frac{1}{3}Mg_3N_2 + \frac{2}{3}LiH + 2H_2 \quad (3)$$

As can be seen from eq 3, a complete conversion of $Li_2Mg(NH)_2$ and $LiBH_4$ at 1:0.67 molar ratio would lead to the highest hydrogen desorption capacity, which was proved in this study (Figure 3). At $x = 0.67$, $LiBH_4$ and $Li_2Mg(NH)_2$ reacted completely and 9.1% hydrogen desorption amount was measured, which was the highest hydrogen desorption amount among the samples studied. At $x > 0.67$, with $LiBH_4$ being in excess with respect to $Li_2Mg(NH)_2$, a lower hydrogen desorption amount was detected. Conversely, when $LiBH_4$ was in deficit ($x < 0.67$), the conversion of $Li_2Mg(NH)_2$ was incomplete, which yielded a lower dehydrogenation amount. Listed in Table 1 are the hydrogen desorption amounts measured in this study and the calculated values for comparison. The temperature 220 °C was chosen on the basis of the TPD curves at the point between the two hydrogen release steps.

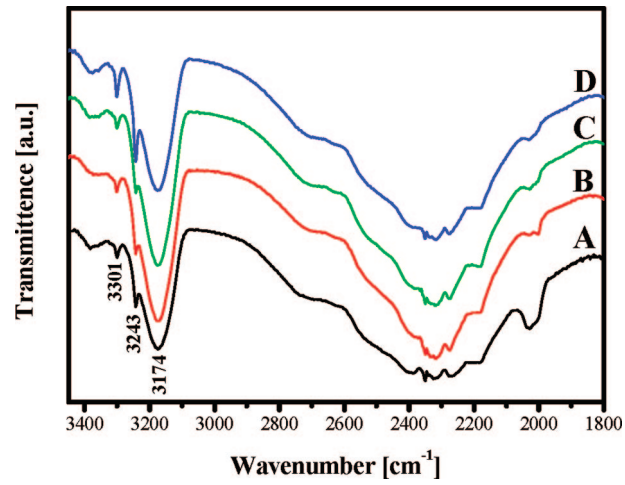

Figure 4. FTIR spectra of samples after desorption to 220 °C: (A) TMS-I, (B) $x = 0.5$, (C) $x = 0.67$, (D) $x = 1.0$.

Table 1. Hydrogen Desorption Amount to 220 °C Following Eq 1 and 320 °C Following Eqs 1 and 3

	first H_2 desorption at 220 °C (wt %)		total H_2 desorption at 320 °C (wt%)	
x	theor.	exp.	theor.	exp.
0.3	5.1	5.0	7.4	7.4
0.5	4.8	4.7	8.4	8.4
0.67	4.6	4.6	9.2	9.1
1.0	4.3	4.2	8.5	8.2

It can be seen the measured values are in good agreement with the calculated ones except for the sample at $x = 1$, which will be discussed in the following section.

Influence of $LiBH_4$ Content on Chemical Composition in Dehydrogenation Process. The FTIR spectra from the samples after the first dehydrogenation step to 220 °C showed the same absorbances for the samples at $x = 0.5$, 0.67 and 1.0 as well as for the TMS-I sample ($1MgH_2-2LiNH_2-1LiBH_4$) (Figure 4). The N−H vibration at 3174 cm^{-1} indicates the formation of the ternary imide $Li_2Mg(NH)_2$. The absorbance at 3243 and 3301 cm^{-1} suggests the existence of $Li_4(BH_4)(NH_2)_3$, which was observed previously in the $LiBH_4$-modified Li−Mg−N−H system after the first desorption step.[15] Nevertheless, the B−H vibration in the range 2200−2400 cm^{-1} seemed unchanged in the desorption process, which was also observed earlier by Chater et al.[18] The FTIR spectra for the samples after the second dehydrogenation step (Figure 5) verified clearly the dependence of the $Li_2Mg(NH)_2$ consumption on its stoichiometric relationships with $LiBH_4$. At $x = 0.5$, $LiBH_4$ was in deficit with respect to $Li_2Mg(NH)_2$, and $LiBH_4$ was fully converted. No absorbance related to B−H bonding in the range 2200−2400 cm^{-1} was detected, whereas the N−H vibration at 3174 cm^{-1} attributed to $Li_2Mg(NH)_2$ was detectable. At $x = 0.67$, where full consumption of both $LiBH_4$ and $Li_2Mg(NH)_2$ was expected, neither B−H nor N−H vibration was observed.

(17) Hu, J. J.; Liu, Y.; Wu, G.; Xiong, Z.; Chen, P. *J. Phys. Chem. C* **2007**, *111*, 18439–18443.

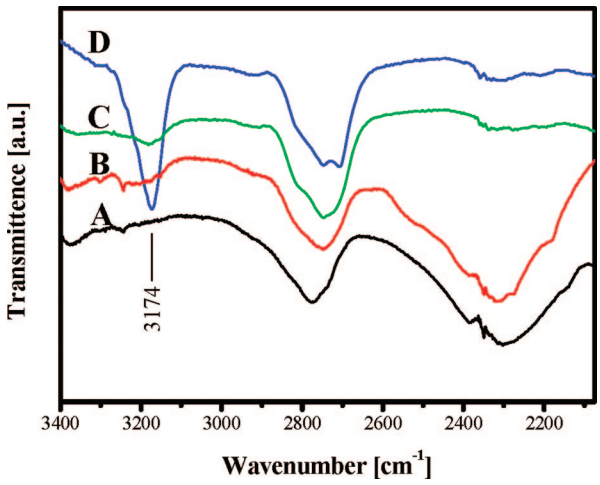

Figure 5. FTIR spectra of samples after desorption to 320 °C: (A) TMS-I, (B) $x = 1.0$, (C) $x = 0.67$, (D) $x = 0.5$.

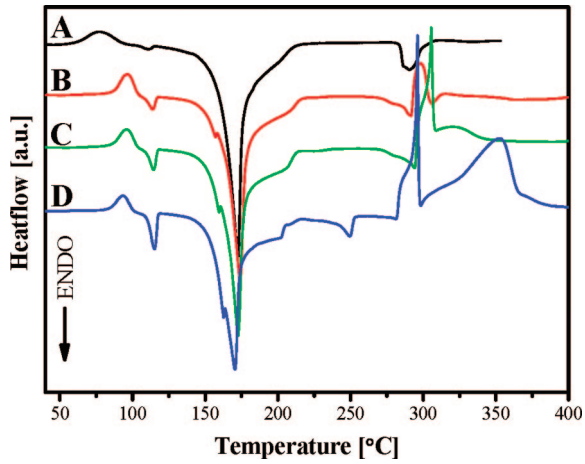

Figure 6. DSC measurements of samples with various $LiBH_4$ contents: (A) $x = 0.3$, (B) $x = 0.5$, (C) $x = 0.67$, (D) $x = 1.0$.

In contrast, for the sample at $x = 1$, no N−H but B−H vibration appeared in the FTIR spectra.

Influence of $LiBH_4$ Content on Heat Effects. The DSC curves of the as-milled samples with different contents of $LiBH_4$ showed slightly decreased peak temperatures with increased $LiBH_4$ content for the hydrogen release in the low temperature range in the proximity of 175 °C (Figure 6). The endothermic peak at 115 °C was due to the first-order phase transition of $LiBH_4$ and its intensity increases with increased $LiBH_4$ content. The exothermic event below 100 °C could be due to the formation of the complexes $(LiNH_2)_x(LiBH_4)_{1-x}$ between $LiBH_4$ and $LiNH_2$ with the latter being generated from the equilibrium of reaction 4, as described in ref 15

$$2LiNH_2 + MgH_2 \leftrightarrow Mg(NH_2)_2 + 2LiH \qquad (4)$$

In addition, there appeared a small endothermic peak from $x = 0.5$ beside the major desorption peak and this peak shifted to higher temperature with increased x value. This peak could be the reverse reaction of the formation of the complexes $(LiNH_2)_x(LiBH_4)_{1-x}$. As the dehydrogenation proceeded, NH_2^- was being consumed, and the complexes $(LiNH_2)_x(LiBH_4)_{1-x}$ had to release $LiNH_2$ to maintain the hydrogen desorption.

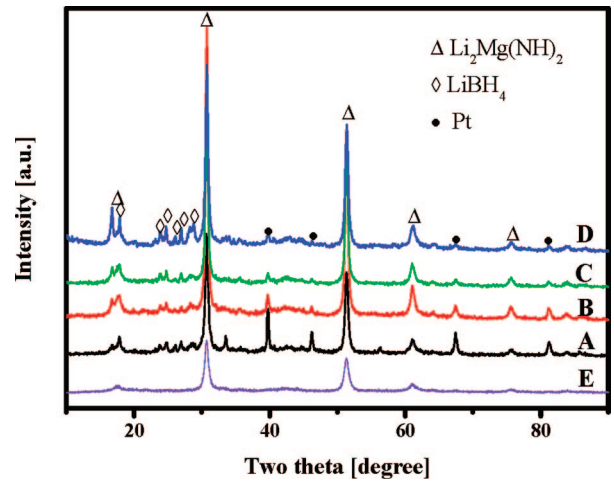

Figure 7. XRD patterns of samples after desorption to 220 °C: (A) TMS-I, (B) $x = 0.5$, (C) $x = 0.67$, (D) $x = 1.0$.

The hydrogen release in the second step exhibited complicated heat effects, from slightly endothermic at $x = 0.3$ via slightly exothermic at $x = 0.5$ to strongly exothermic at $x = 1.0$. From the FTIR results above, part of $LiBH_4$ has been converted to $Li_4(BH_4)(NH_2)_3$, which persisted after the first dehydrogenation. The second hydrogen release in the high temperature range may presumably become a reaction of $Li_4(BH_4)(NH_2)_3$ or unconverted $LiBH_4$ with $Li_2Mg(NH)_2$. For samples at $x = 0.67$ or lower, the reaction between $Li_2Mg(NH)_2$ and $Li_4(BH_4)(NH_2)_3$ may be dominating. For the sample at $x = 1$ and $1MgH_2$-$2LiNH_2$-$1LiBH_4$, $LiBH_4$ was in excess. In this case, $Li_2Mg(NH)_2$ may preferably react with $LiBH_4$ at first. As a consequence, $Li_4(BH_4)(NH_2)_3$ or its analogues formed in the first dehydrogenation step remained unreacted. The quaternary hydrides of $(LiNH_2)_x$-$(LiBH_4)_{1-x}$ decompose strongly exothermically in the 300−380 °C temperature range (see the Supporting Information), which could be a reason for the strong heat effects for samples with excess in $LiBH_4$. In addition, the decomposition of $Li_4(BH_4)(NH_2)_3$ was accompanied by escalated ammonia generation, as observed in this study (Figure 2). With ammonia generation, lower values of hydrogen desorption will be recorded by the Sieverts' system, which accounts for the lower hydrogen release amount for the sample at $x = 1$ (Table 1). The exothermic heat effects predict that the second dehydrogenation step may not be reversible.

Influence of $LiBH_4$ content on Phase Changes in Dehydrogenation Process. Depending on the dehydrogenation process, different crystal structures of $Li_2Mg(NH)_2$ can be formed.[17] The dehydrogenation to 220 °C resulted in the formation of $Li_2Mg(NH)_2$ with cubic structure[6,13,17] for all the studied samples (Figure 7). Residues of unreacted $LiBH_4$ was also detected. The quaternary hydride observed by FTIR was not detected, possibly because of low content. The Pt pattern was caused by the Pt sample holder. After the second dehydrogenation step, Mg_3N_2 and Li_3BN_2 were observed for the studied samples (Figure 8), consistent with the observations in the ref 13 on TMS-I. In addition, the

(18) Chater, P. A.; David, W. I. F.; Johnson, S. R.; Edwards, P. P.; Anderson, P. A. *Chem. Commun.* **2006**, 2439–2441.

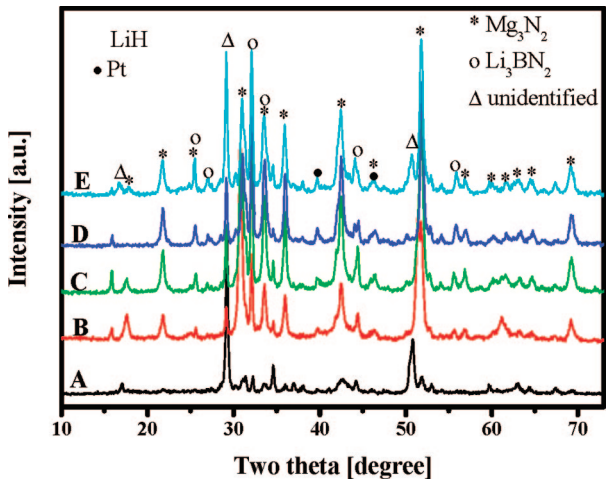

Figure 8. XRD patterns of samples after desorption to 320 °C: (A) TMS-I, (B) $x = 0.3$, (C) $x = 0.5$, (D) $x = 0.67$, (E) $x = 1.0$.

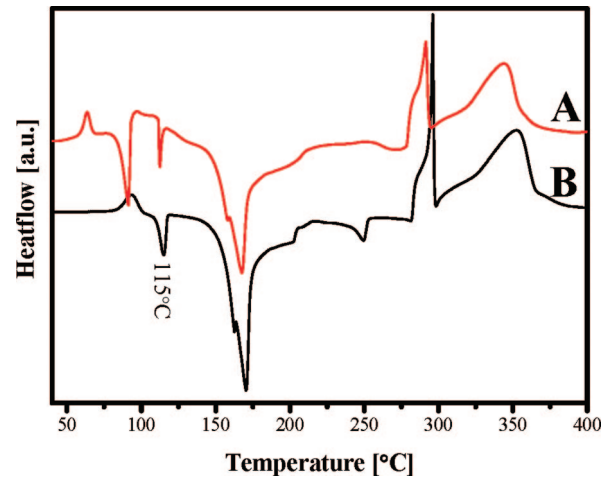

Figure 10. DSC measurements: (A) TMS-I and (B) 1Mg(NH$_2$)$_2$−2LiH−1LiBH$_4$ ($x = 1$).

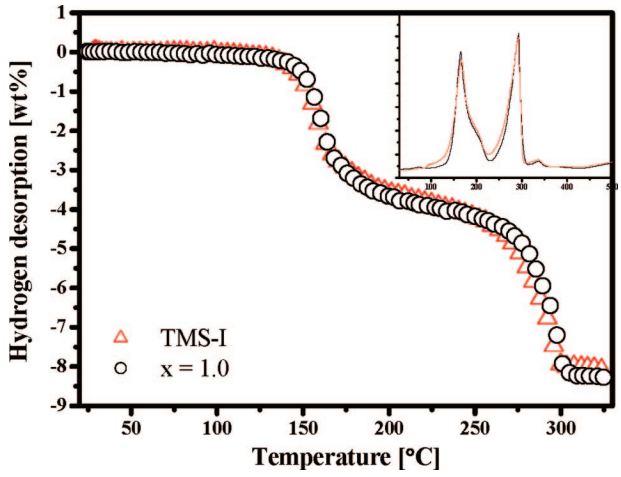

Figure 9. Volumetric hydrogen release of TMS-I and 1Mg(NH$_2$)$_2$−2LiH−1LiBH$_4$ ($x = 1$).

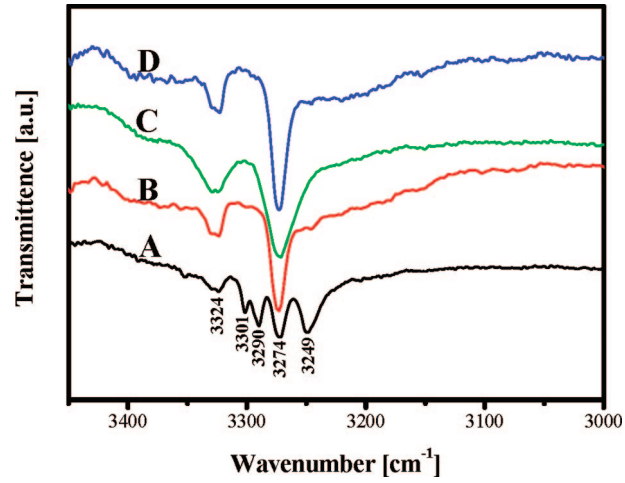

Figure 11. FTIR spectra: (A) TMS-I as-milled; (B) TMS-I annealed at 120 °C for 20 min; (C) $x = 1$ as-milled; (D) $x = 1$ annealed at 120 °C for 20 min.

diffraction peaks at 16.8, 29.2, 34.5, and 51 did not originate from known structures in the reference database, but could be a new phase with composition similar to LiMgBN$_2$.[13]

Comparison of 1Mg(NH$_2$)$_2$−2LiH−1LiBH$_4$ System with 1MgH−2LiNH$_2$−1LiBH$_4$ System. By plotting the volumetric measurements of the sample TMS-II at $x = 1.0$ and the TMS-I sample (1MgH$_2$−2LiNH$_2$−1LiBH$_4$) (Figure 9), a very similar behavior in hydrogen desorption can be seen; 8.2 wt % hydrogen desorption was detected for $x = 1.0$, which coincides with the amount reported for the MgH$_2$−LiNH$_2$−LiBH$_4$ mixture at a 1:2:1 molar ratio.[13] The TPD curves of the Mg(NH$_2$)$_2$−2LiH−1LiBH$_4$ ($x = 1$) and the 1MgH$_2$−2LiNH$_2$−1LiBH$_4$ system in the insertion of Figure 9 display the same peak position and intensity as well.

The DSC measurement of the as-milled TMS-I sample shows the same peak temperature and heat effects in the first and the second dehydrogenation as those of the sample at $x = 1$ (Figure 10), which indicates that the conversion of MgH$_2$ and LiNH$_2$ to Mg(NH$_2$)$_2$ and LiH in reaction 4 may have been accomplished before the first-step dehydrogenation. The endothermic peak followed by the baseline uplift (exothermic) of the TMS-I samples prior to the first dehydrogenation step may be related to the conversion reaction.

For the FTIR spectra, only N−H stretching at 3272 and 3326 cm^{-1} originated from Mg(NH$_2$)$_2$ appeared from the sample of $x = 1$ (Figure 11). In contrast, multiple absorbance peaks in the range 3200−3400 cm^{-1} were observed for the as-milled TMS-I sample (1MgH$_2$−2LiNH$_2$−1LiBH$_4$). While two of the multiple absorbance peaks at 3272 and 3326 cm^{-1} can be attributed to the N−H vibration of Mg(NH$_2$)$_2$, the other three peaks hint at in situ formation of solid solutions or quaternary hydrides from LiNH$_2$ and LiBH$_4$. LiNH$_2$ and LiBH$_4$ have been reported to form stable complexes of Li$_2$(BH$_4$)(NH$_2$) and Li$_4$(BH$_4$)(NH$_2$)$_3$ at 1:1 and 3:1 molar ratios, respectively.[18−22] On the basis of the DSC analysis, the TMS-I sample was annealed for 20 min at 120 °C, which was the temperature between the phase transition of LiBH$_4$ and the first dehydrogenation step. We obtained an FTIR spectrum from the annealed sample identical to

(19) Meisner, G. P.; Scullin, M. L.; Balogh, M. P.; Pinkerton, F. E.; Meyer, M. S. *J. Phys. Chem. B* **2006**, *110*, 4186–4192.
(20) Filinchuk, Y. E.; Yvon, K.; Meisner, G. P.; Pinkerton, F. E.; Balogh, M. P. *Inorg. Chem.* **2006**, *45*, 1433–1435.
(21) Chater, P. A.; Anderson, P. A.; Prendergast, J. W.; Walton, A.; Mann, V. S. J.; Book, D.; David, W. I. F.; Johnson, S. R.; Edwards, P. P. *J. Alloys Compd.* **2007**, *446−447*, 350–354.
(22) Chater, P. A.; David, W. I. F.; Anderson, P. A. *Chem. Commun.* **2007**, 4770–4772.

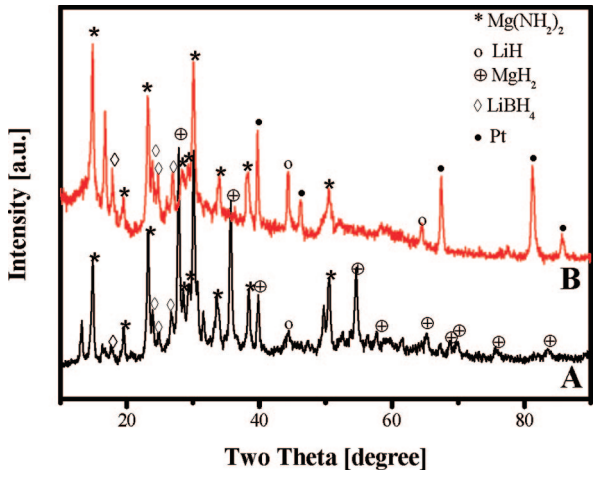

Figure 12. XRD patterns of as-milled samples: (A) TMS-I and (B) $1Mg(NH_2)_2-2LiH-1LiBH_4$ ($x = 1$).

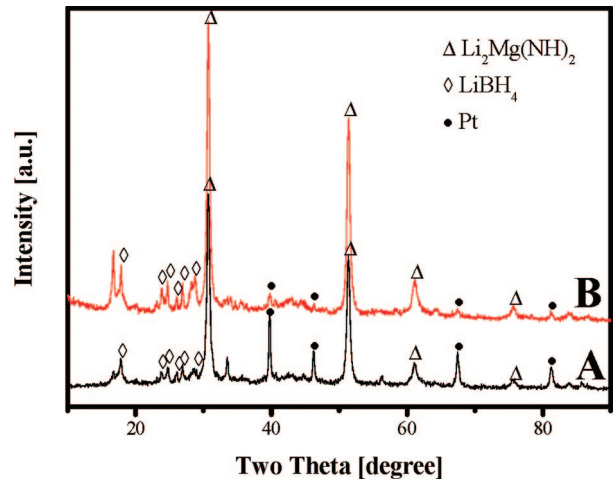

Figure 13. XRD patterns of samples desorbed to 220C: (A) TMS-I and (B) $1Mg(NH_2)_2-2LiH-1LiBH_4$ ($x = 1$).

the spectrum of as-milled sample at $x = 1$ (Figure 11), whereas the absorbance at 3243/3301 cm^{-1} attributed to $Li_4(BH_4)(NH_2)_3$ disappeared completely. This means the conversion to the new amide−hydride pair occurred at the expense of the quaternary hydrides.

An extra sample was prepared at a molar ratio of 1:2 for MgH_2 and $LiNH_2$ under the same milling conditions without $LiBH_4$ in order to know whether the conversion reaction 4 can take place during ball milling. Only a weak shoulder absorbance related to $Mg(NH_2)_2$ was discernible (see the Supporting Information) and the subsequent tempering at 120 °C for 20 min after ball milling did not promote the metathesis. A partial conversion from MgH_2 and $LiNH_2$ to $Mg(NH_2)_2$ and LiH was realized previously by Luo and Sickafoose by heating the ball-milled mixture of MgH_2 and $LiNH_2$ to 220 °C for 2 h under 100 bar H_2 pressure.[23] It is obvious that the presence of $LiBH_4$ facilitated the conversion.

$Mg(NH_2)_2$ usually becomes amorphous upon ball milling.[24] However, the starting components ($Mg(NH_2)_2$, LiH and $LiBH_4$) of the sample at $x = 1.0$ could still be detected by XRD (Figure 12A) after ball milling. Surprisingly, prevailing diffraction peaks of $Mg(NH_2)_2$ and LiH were observed in the as-milled TMS-I sample ($1MgH_2-2LiNH_2-1LiBH_4$) besides the patterns of its starting chemicals of MgH_2 and $LiBH_4$ (Figure 12B), which confirmed the partial formation of $Mg(NH_2)_2$ and LiH during the ball-milling process. Although $Li_4(BH_4)(NH_2)_3$ was detected in the as-milled $1MgH_2-2LiNH_2-1LiBH_4$ sample by FTIR (Figure 11), it disappeared in the conversion process and was recovered after hydrogen desorption to 220 °C (Figure 4). In addition, both samples showed cubic structure $Li_2Mg(NH)_2$ XRD patterns together with the unreacted $LiBH_4$ (Figure 13) after the first dehydrogenation step to 220 °C.

Combining the above results, it is clear that the introduction of $LiBH_4$ enabled the conversion from MgH_2 and $LiNH_2$ to $Mg(NH_2)_2$ and LiH before hydrogen desorption, which makes the ternary mixture $1MgH_2-2LiNH_2-1LiBH_4$ an equivalent to $Mg(NH_2)_2-2LiH-1LiBH_4$ as a hydrogen storage material. As pointed out in our previous work, no $Li_2Mg(NH)_2$ as "seeds" was available with the $1Mg(NH_2)_2-2LiH-1LiBH_4$ system, the enhancing effect of $LiBH_4$ on the Li−Mg−N−H system could arise from factors other than seeding effect. Although the persistence of $Li_4(BH_4)(NH_2)_3$ in the material may provide a clue for the effects of $LiBH_4$, a sample specially prepared by adding 0.3 mol $Li_4(BH_4)(NH_2)_3$ to the $1Mg(NH_2)_2-2LiH$ mixture did not show improvement in the desorption kinetics (see the Supporting Information). Investigations with addition of $LiBD_4$ instead of $LiBH_4$ are underway in order to clarify whether there is interaction between D^- in the BD_4^- anion and H^+ in the NH_2^- anion.

Conclusions

By introducing $LiBH_4$ to the $Mg(NH_2)_2-LiH$ (1:2 molar ratio) system, a maximum hydrogen amount of 9.1 wt % was obtained at 300 °C for the composition $1Mg(NH_2)_2-2LiH-0.67LiBH_4$. Various characterizations revealed that the mixture of MgH_2 and $LiNH_2$ was converted to $Mg(NH_2)_2$ and LiH below 120 °C in the presence of $LiBH_4$. A comparison between the sample $1Mg(NH_2)_2-2LiH-1LiBH_4$ and the ternary mixture $1MgH_2-2LiNH_2-1LiBH_4$ indicated that both samples behave very similarly in hydrogen desorption, thermal effects, and structural changes during dehydrogenation.

Acknowledgment. The authors thank the EU-IP "Nanolty" (Contract No. 210092) for financial support.

Supporting Information Available: (1) DSC curves of quaternary hydrides; (2) FTIR spectra of as-ball milled and annealed $1MgH_2$-$2LiNH_2$; (3) Hydrogen desorption Isotherms of $1Mg(NH_2)_2$-2LiH and $1Mg(NH_2)_2$-2LiH-$0.3Li_4(BH_4)(NH_2)_3$ at 140 °C (PDF). This material is available free of charge via the Internet at http://pubs.acs.org.

CM802129B

(23) Luo, W. F.; Sickafoose, S. *J. Alloys Compd.* **2006**, *407*, 274–281.
(24) Hu, J. J.; Wu, G.; Liu, Y.; Xiong, Z.; Chen, P.; Murata, K.; Sakata, K.; Wolf, G. *J. Phys. Chem. B* **2006**, *110*, 14688–14692.